Acta Materialia 132 (2017) 222–229

Contents lists available at ScienceDirect

Acta Materialia

journal homepage: www.elsevier.com/locate/actamat

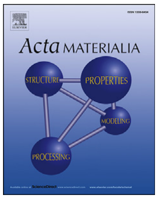

Full length article

Microstructural and magnetic properties of Mn-Fe-P-Si (Fe$_2$ P-type) magnetocaloric compounds

Maximilian Fries [a], [*], Lukas Pfeuffer [a], Enrico Bruder [b], Tino Gottschall [a], Semih Ener [a], Léopold V.B. Diop [a], Thorsten Gröb [b], Konstantin P. Skokov [a], Oliver Gutfleisch [a], [**]

[a] *Funktionale Materalien, Fachbereich Materialwissenschaft, TU Darmstadt, 64287, Darmstadt, Germany*
[b] *Physikalische Metallkunde, Fachbereich Materialwissenschaft, TU Darmstadt, 64287, Darmstadt, Germany*

ARTICLE INFO

Article history:
Received 1 February 2017
Received in revised form
18 April 2017
Accepted 18 April 2017
Available online 21 April 2017

Keywords:
Magnetocalorics
Magnetism
Intermetallic phases
Transition metals
Phase transition
Phase composition

ABSTRACT

Fe$_2$ P-based magnetocaloric compounds are an important and industrially relevant material class for magnetic refrigeration, yet their microstructure and its influence on the magnetic properties is hardly discussed in literature. We prepared Mn-Fe-P-Si-based samples using a powder metallurgical process and analyzed their microstructural and thermomagnetic properties. XRD, SEM, EDX and EBSD analysis reveal a phosphorous depleted cubic secondary phase in many samples with distinct microstructural properties giving an insight into the phase formation process. A porous morphology was found, hindering the direct application of the materials a magnetocaloric heat exchanger in bulk-like structures. The “virgin” effect could be in-situ observed for the first time on a macroscopic scale using temperature-dependent optical microscopy. Thermomagnetic measurements reveal a difference in transition temperature T_t in comparison to literature values which is attributed to a processing induced deviation from the nominal composition. The isothermal entropy change ΔS_T and adiabatic temperature change ΔT_{ad} were studied as well as their cyclic behavior. The effect of secondary phases is discussed and the importance of the metal/non-metal (M/NM)-ratio is shown. The article presents a road map for the preparation of Mn-Fe-Si-P-based alloys with highest quality.

1. Introduction

Modern society is in an ever increasing need of easily available and environmentally friendly cooling technologies. A nearly exponential increase in demand of cooling power is predicted for the next 50 years especially for household refrigeration and air conditioning [1]. In large scale cooling devices the use of ozone layer depleting chlorofluorocarbons is still current practice, whereas small scale conventional compressor based cooling technologies nowadays rely on non-ozone depleting, yet highly explosive hydrofluorocarbons which show an about thousand times higher global warming potential than for example CO$_2$ [2–4]. A solid refrigerant based technology like magnetocaloric cooling could overcome these issues. Furthermore, the efficiency of these type of devices is expected to exceed the efficiency of vapor compression based technology leading to a much reduced energy consumption compared to conventional technologies [5].

Magnetic refrigeration is based on the magnetocaloric effect which manifests itself in the temperature change of a magnetic material when magnetized or demagnetized. Since the discovery of the magnetocaloric effect in nickel in 1917 by Weiss and Picard [6,7], various magnetocaloric materials have been extensively studied. Followed by the discovery of the giant magnetocaloric effect in Gd$_5$(Si$_x$Ge$_{1-x}$)$_4$ [8] many other promising material systems have been discovered such as La-Fe-Si [9–11], Heusler alloys [12–14] and Fe$_2$ P based alloys [15].

The class of Fe$_2$ P-type compounds adopt the hexagonal Fe$_2$ P-type crystal structure, space group P$\overline{6}$2m. The parent compound displays strong magnetocrystalline anisotropy with the c-axis being the easy magnetization direction. The Fe$_2$ P compound undergoes a transition from a ferromagnetically ordered to a paramagnetic state at 217 K. Linear thermal expansion studies reveal that the ferromagnetic to paramagnetic transition is accompanied by a step-like change in the unit cell volume of 0.05% [16,17]. By substituting Mn on the Fe sites and X-elements (X: As,

---

[*] Corresponding author.
[**] Corresponding author.

E-mail addresses: fries@fm.tu-darmstadt.de (M. Fries), gutfleisch@fm.tu-darmstadt.de (O. Gutfleisch).

http://dx.doi.org/10.1016/j.actamat.2017.04.040
1359-6454/

Ge, Si, B) on the P sites, the magnetocaloric properties can be adjusted [18–26]. The system shows magnetization and entropy changes comparable to other candidate materials for magnetic refrigeration and the properties are tunable around room temperature.

The most promising composition from an application point of view is $(Mn,Fe)_{1.95}(P,Si)$, as it contains no critical, expensive and toxic elements [27]. It was shown that by varying the content of Fe and Si, the transition can be tuned in a wide temperature range and hysteresis can be minimized by carefully adjusting the composition [18,20,22,25]. The compounds are usually synthesized via a powder metallurgical route and a solid state reaction or by pyro metallurgical processes like for example melt-spinning [28].

Despite the extensive studies on this series of compounds hardly any investigation on how the microstructure and the occurrence of secondary phases influence the main magnetic and magnetocaloric properties has been published. This is the main focus of our article.

2. Experimental details

Polycrystalline samples with Fe_2 P-type structure were produced by a powder metallurgical route followed by an annealing step. Powders of high purity (≥99.9%) Mn, Fe_2 P, Si and P (total amount 5 g) were mixed in inert atmosphere. In order to compensate evaporation losses, additional P was added to the stochiometric composition. Milling was performed using a Spex 8000 D high-energy ball mill at 875 cycles/min for 80 min in a hardened steel vial with 2 hardened steel balls and a ball to powder ratio of 3.34. The ball-milled powders were uni-axially compacted in a press-form with 0.1 GPa pressure at room temperature. The green-bodies were wrapped in Molybdenum foil and sintered in a vacuum tube furnace under a constant Ar pressure of 1.25 bar for 2 h at 1373 K followed by a 20 h annealing step at 1123 K and slow cooling to room temperature. Prior to all measurements, the surface layers of the sample were ground off in order to remove possible surface oxidation. The list of samples discussed in this article is given in Table 1.

Room temperature powder x-ray diffraction (XRD) measurements were carried out on a Stadi P diffractometer by using Mo $K\alpha_1$ x-ray radiation and a Ge (111) monochromator. Data analysis was performed using the FULLPROF software package [29]. A Tescen high resolution scanning electron microscopy (SEM) equipped with an energy-dispersive x-ray (EDX), back-scatter electron (BSE) and electron back-scatter diffraction (EBSD) detector was used for microstructural characterization. The stoichiometry of the compounds presented in this article were determined by EDX with an error of less than 2 at%. Prior to all magnetic measurements, the materials were cycled 3 times in liquid nitrogen with subsequent heating to room temperature in order to remove the "virgin" effect if not mentioned otherwise. Magnetization measurements were performed using commercial vibrating sample magnetometers, Lake Shore 7400 Series and Quantum Design PPMS-14. For the $M(T)$ measurements, a sweeping rate of 2 K min^{-1} was used, if not mentioned otherwise. The adiabatic temperature change was measured with a purpose built experimental setup which has been described previously [30]. Temperature-dependent optical microscopy was performed on a Zeiss Imager D2.m microscope equipped with a LN_2 cryostat from evico magnetics as described in Ref. [31].

3. Structural and microstructural characterization

The synthesized $Mn_{1.32}Fe_{0.71}P_{0.5}Si_{0.56}$ sample was found to be mainly single phase according to the x-ray diffraction investigation in Fig. 1. The XRD pattern indicates the presence of residual traces of the pseudo-binary cubic $Fm\overline{3}m$ compound $(Mn,Fe)_3$ Si with the composition $Mn_{1.49}Fe_{1.35}$ Si as minority impurity phase. The P-62 m (#189) space group symmetry for $Mn_{1.32}Fe_{0.71}P_{0.5}Si_{0.56}$ could be confirmed. It is worth recalling that earlier published studies also reported the difficulty to synthesize the pure compound [19,21]. The refined unit cell parameters for $Mn_{1.32}Fe_{0.71}P_{0.5}Si_{0.56}$ are a = 6.099(X) Å and c = 3.446(X) Å, which are in good agreement with previously reported values [20,21,32,33].

The BSE image in Fig. 2a) shows the porosity of the samples. The black spots in the BSE image correspond to the pores which are occurring during the formation of the Fe_2 P-phase from the initial powder mixture and they are remaining during the rest of the production route. This porous structure is inevitable and could not be overcome by comparable powder metallurgical routes that are regularly used as described in literature [33]. Therefore, it is hindering a direct application of the material in bulk-like regenerator structures, like plates or channel structures because of their brittleness.

The density of the Mn-Fe-P-Si sample was determined to be

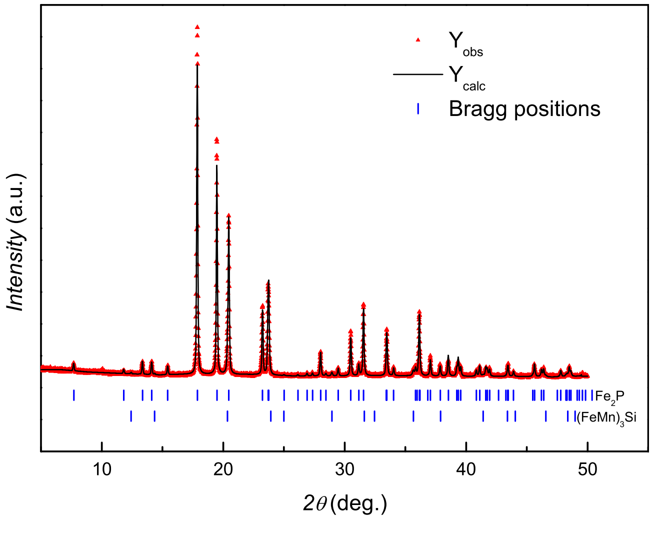

Fig. 1. Room temperature XRD pattern of $Mn_{1.32}Fe_{0.71}P_{0.5}Si_{0.56}$ crystallized in the Fe_2 P structure with traces (<3 wt%) of a $(Fe,Mn)_3$ Si secondary phase.

Table 1
List of samples discussed in the article. The sample names and their corresponding stoichiometry from EDX are given in the first two columns. Eventual secondary phases as well as their weight fractions are in columns three and four. In the last column the M/NM ratios are shown.

Sample ID	Composition main-phase	Composition secondary-phase	wt% secondary phase	M/NM
Sample 1 (S1)	$Mn_{1.32}Fe_{0.71}P_{0.5}Si_{0.56}$	$Mn_{1.49}Fe_{1.35}Si$	5	1.93
Sample 2 (S2)	$Mn_{1.24}Fe_{0.70}P_{0.5}Si_{0.58}$	–	0	1.80
Sample 3 (S3)	$Mn_{1.19}Fe_{0.68}P_{0.5}Si_{0.57}$	$Mn_{1.32}Fe_{1.21}Si$	3	1.75
Sample 4 (S4)	$Mn_{1.13}Fe_{0.59}P_{0.5}Si_{0.52}$	$Mn_{1.33}Fe_{1.16}Si$	6	1.67
Sample 5 (S5)	$Mn_{1.20}Fe_{0.68}P_{0.5}Si_{0.66}$	–	0	1.62
Sample 6 (S6)	$Mn_{1.22}Fe_{0.59}P_{0.5}Si_{0.59}$	–	0	1.73